AIP Journal of Applied Physics

Small angle x-ray and neutron scattering study of disordered and three dimensional–ordered magnetic protein arrays

O. Kasyutich, D. Tatchev, A. Hoell, F. Ogrin, C. Dewhurst et al.

Citation: J. Appl. Phys. **105**, 07B528 (2009); doi: 10.1063/1.3075865

View online: http://dx.doi.org/10.1063/1.3075865

View Table of Contents: http://jap.aip.org/resource/1/JAPIAU/v105/i7

Published by the AIP Publishing LLC.

Small angle x-ray and neutron scattering study of disordered and three dimensional–ordered magnetic protein arrays

O. Kasyutich,[1,a] D. Tatchev,[2,3] A. Hoell,[2] F. Ogrin,[4] C. Dewhurst,[5] and W. Schwarzacher[1]
[1]*H.H. Wills Physics Laboratory, University of Bristol, Bristol BS8 1TL, United Kingdom*
[2]*Helmholtz Centre for Materials and Energy, 14109 Berlin, Germany*
[3]*Institute of Physical Chemistry, 1113 Sofia, Bulgaria*
[4]*School of Physics, University of Exeter, Exeter EX4 4QL, United Kingdom*
[5]*Institute Laue-Langevin, BP 156, 38042 Grenoble, France*

(Presented 13 November 2008; received 19 September 2008; accepted 16 December 2008; published online 1 April 2009)

The magnetic nanoparticles of Fe_3O_4-γ–Fe_2O_3 grown inside the cavity of globular proteins (apoferritin)-magnetoferritin proved to be a useful model system for studying the fundamental effects of magnetostatic interactions in nanoparticle assemblies. In this work the main focus is on structural characterization of such new nanocomposites by small angle x-ray scattering (SAXS) and small angle neutron scattering to evaluate interparticle separation (center to center) in two types of assemblies: three dimensional periodic arrays and disordered (amorphous) assemblies. Straightforward analysis of the face-centered cubic pattern of periodic arrays revealed that the interparticle spacing is 9.9 nm, whereas the SAXS pattern of disordered assembly reveals three correlation lengths, one of which is 10.5 nm and corresponds to the interparticle (center-to-center) nearest neighbor distance. The magnetic behaviors of the two systems are distinctly different. Given that the interparticle separation differs by only ~0.6 nm, the main structural factor contributing to the observed differences in magnetic properties is likely to be the array order. © *2009 American Institute of Physics*. [DOI: 10.1063/1.3075865]

I. INTRODUCTION

The magnetic behavior of nanoparticle assemblies is a topic of intense research in nanomagnetism. One of the fundamental questions[1–3] is the interplay between interparticle separation, spatial order, and the effect of those parameters on magnetic properties for magnetostatically interacting systems.

Magnetoferritin is a well studied[4–6] system of isolated homogeneous magnetic nanoparticles with potential applications in biomedicine.[7] It consists of nanodimensional particles of ferrimagnetic Fe_3O_4-γ–Fe_2O_3 (magnetite/maghemite) encased in a spherical protein shell with conserved dimensions (8 nm internal diameter and 2 nm shell thickness). Recently[8] we demonstrated that dipolar interactions lead to both a decrease in the peak energy and a broadening of the (effective) energy barrier distribution in a system of interacting magnetoferritin nanoparticles arranged into a dense disordered array. These experimental findings were in good agreement with theory.[9]

However the true benefit of having these nanoparticles encased in the protein becomes apparent once protein crystallization is applied to generate large three dimensionally ordered arrays. In a recent paper[10] we described this new approach in which the periodicity and symmetry of the array is controlled solely by the protein. It was shown experimentally[10] and theoretically[11] that the magnetic behavior of such assemblies differs significantly from that of their noninteracting counterparts. Nevertheless the question of whether interparticle spacing or nanoparticle ordering induces such differences requires further clarification. In this paper the main objective is to compare the structure and magnetic behavior of three dimensional (3D) crystals with dimensions of a few hundreds of micrometers to those of dense disordered 3D assemblies of the same nanoparticles.

II. EXPERIMENTAL METHODS

First, Fe_3O_4-γ–Fe_2O_3 nanoparticles were synthesized inside apoferritin protein biotemplates via well established protocols.[6] The synthesized nanoparticles were characterized by transmission electron microscopy, as described earlier.[8] Postsynthesis purification with ion-exchange chromatography column was followed by low field/high gradient magnetic separation, similar to a procedure[12] used to separate water soluble magnetic Fe_3O_4 nanoparticles. Finally, protein monomers (each carrying a single crystal magnetic core) were crystallized to form a 3D periodic array. The details of this method have been described earlier.[10] Additionally, a disordered 3D assembly was produced by adding precipitating agent ($CdSO_4$) and altering the *p*H of the electrolyte. These two types of assemblies were extracted from the mother liquor, washed, and left to dry in air. Dry 3D periodic arrays (crystals) and glasslike assemblies (pellet) were mounted on Kapton tape and characterized magnetically and by small angle scattering techniques—small angle x-ray scattering (SAXS) and small angle neutron scattering (SANS).

Characterization of the nanostructure of both samples was performed by SAXS at the 7T-MPW-SAXS beamline at the Helmholtz Centre Berlin for Materials and Energy

[a]Electronic mail: oksana.kasyutich@bristol.ac.uk.

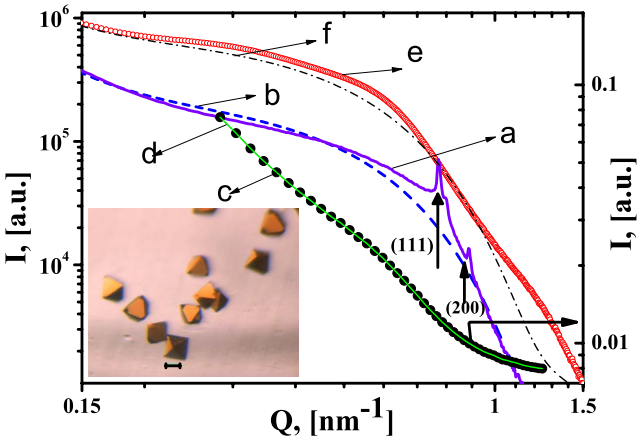

FIG. 1. (Color online) Small angle scattering intensities as a function of Q: experimental SAXS curve of crystalline 3D assembly of magnetoferritin (a) with fitted form factor (b); experimental SAXS (e) and SANS (c) curves of disordered 3D assembly with fitted form factor—(f) (for SAXS) and (d) (for SANS). Only curves (c) and (d) (SANS) are related to the Y-axis to the right, as indicated by arrow. Inset: a typical optical image of 3D arrays (crystals) of magnetoferritin monomers. Each crystal is an ordered 3D array of magnetic nanoparticles formed by growing magnetite-maghemite cores inside apoferritin shells and subsequently crystallizing the protein. The scale bar is 100 μm.

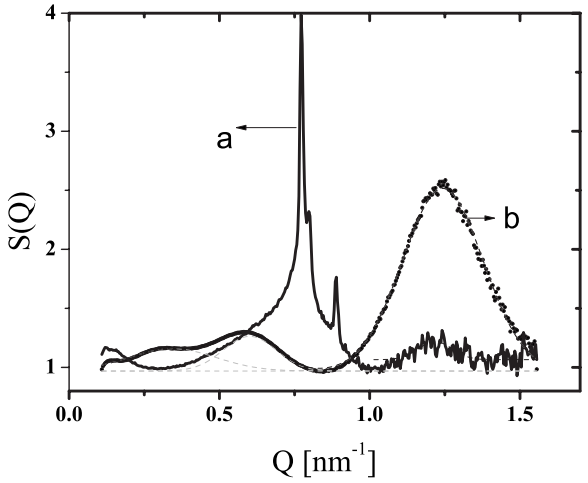

FIG. 2. Calculated structure factors for the magnetoferritin crystal (a) and the amorphous pellet (b). Solid lines are guides for the eyes. Dashed lines are Gauss-peak fits.

(BESSY). The one dimensional SAXS scattering curves were obtained by circularly averaging two dimensional patterns from a charge coupled device camera. An Ag behenate standard sample was used to find the x-ray beam center and for calibration of the magnitude of the scattering vector.

SANS data were collected at the D22 beamline at the Institut Max von Laue–Paul Langevin (ILL) in Grenoble, France. Due to the small volume of the sample available and correspondingly poor magnetic scattering data obtained so far, the results presented here concern only the structural characterization of the disordered assembly. The measurement was taken at room temperature with the sample-detector distance fixed at 4 m. The hysteresis loops were measured using a Quantum Design superconducting quantum interference device magnetometer.

III. RESULTS AND DISCUSSION

The SAXS results for dry magnetoferritin crystals are presented in Fig. 1(a). Two peaks at 0.778 and 0.892 nm^{-1} correspond to the (111) and (200) reflections of a fcc crystal lattice with lattice parameter $a=14.06$ nm. The shortest interparticle distance (center to center) is therefore 9.94 nm.

The scattered intensity from a system of monodisperse nanoparticles of the same shape is described by[13,14] $I(Q)=F(Q)^2S(Q)^2$ (*), where Q is the magnitude of the scattering vector; $F(Q)$ is the form factor, accounting for the structure of individual nanoparticles; and $S(Q)$ is the structure factor, accounting for the x-ray interference from neighboring particles. All scattering curves presented in Fig. 1 contain several features which are typical of small angle scattering from systems of nanoparticles: constant background scattering at high Q values, best seen on the SANS curve [Fig. 1(c), closed circles; and Porod-type scattering proportional to Q^{-4} that appears at smallest Q values, again best visible on the SANS curve, but present in all SAS curves. To estimate $F(Q)$ the following assumptions were made: (1) for a crystal sample $S(Q)\rightarrow 1$ when Q is outside the crystal structure Bragg peaks' range; and (2) a spherical core-shell particle was assumed and log-normal particle size distribution was taken into account. The fitted dashed line in Fig. 1(b) is a proposed form factor. The obtained fitted value of the radius of magnetite/maghemite core is 2.73 ± 0.3 nm, surrounded by 1.4 ± 0.2 nm thick (dehydrated) protein shell. The variance of the distribution is 0.301 nm^2 and 90% of the particle radii lie between 2 and 4 nm. A similar average radius of 2.7 nm for magnetic nanoparticles in the dry pellet was derived from superparamagnetic magnetization curves, measured at 273 K, using the Langevin function fit to the data. The SANS form factor [Fig. 1(d), solid line] fits very well to the experimental SANS curve [Fig. 1(c)] and qualitatively matches the experimental SAXS curve [Fig. 1(e)] and SAXS form factor [Fig. 1(f)] of the disordered sample, providing that the difference in scattering intensity and ratios between $F(Q)$, the Porod type and background scattering is taken into account. We interpret the deviation of the experimental SAXS curve for the disordered assembly from the fitted $F(Q)$ as the structural contribution to the x-ray scattering curve. Therefore, by dividing the experimental x-ray scattering curves by their fitted $F(Q)$, the structure factors for the crystal and amorphous assembly were obtained [Figs. 2(a) and 2(b)].

The calculated structure factor of the crystal assembly [Fig. 2(a)] agrees well with the peaks on the experimental scattering curve; only their positions are slightly shifted. This changes the lattice parameter to $a=14.11\pm0.02$ nm, which is within the experimental error. The calculated structure factor of the amorphous sample shows broad peaks [Fig. 2(b), solid line as guide for the eyes], which are typical of an amorphous material. The strongest peak at 1.24 ± 0.01 nm^{-1} correlates well with the 1.22 nm^{-1} peak on the calculated structure factor curve of the crystal assembly [Fig. 2(a)]. This gives a scattering correlation length of 5.1–5.2 nm, which is very close to the diameter of the magnetic nanoparticles and is most likely associated with scattering from the inorganic cores. Additional peaks appear at $Q=0.34\pm0.02$

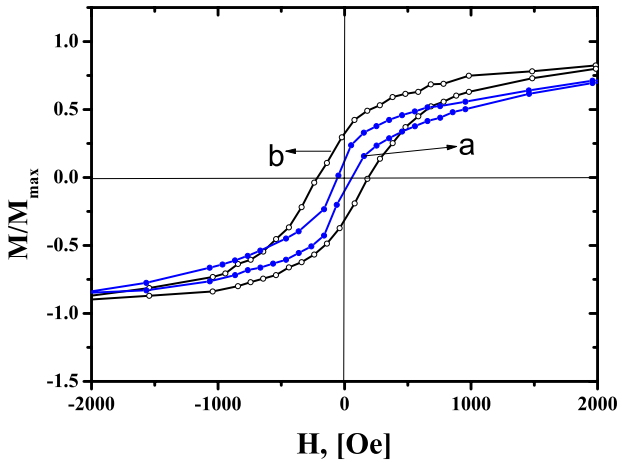

FIG. 3. (Color online) Hysteresis loops for an ordered fcc array of magnetoferritin (a) and disordered assembly of magnetoferritin (b), measured at 10 K.

and 0.60 ± 0.01 nm^{-1}, which gives rise to scattering correlation lengths of 19 ± 1 and 10.5 ± 0.2 nm for the amorphous sample. The latter corresponds to the nearest interparticle distance, and there is a weak indication of longer range correlation length.

In this experiment the magnetic behaviors of both 3D periodic assembly of nanoparticles with interparticle separation of 9.94 nm and disordered assembly with average interparticle separation of 10.5 nm evaluated by SAXS were compared at 10 K. It is clear that the coercive force and magnetic remanence of the ordered arrays [Fig. 3(a)] are much smaller than in the case of the disordered assembly [Fig. 3(b)]. Earlier we reported[10] the magnetic properties of fcc arrays of magnetoferritin in comparison with a suspension of noninteracting monomeric magnetic proteins. The spatial separation between the nanoparticles in the fcc array was almost an order of magnitude smaller than in the dilute suspension (~ 10 nm compared to ~ 100 nm). Therefore decreased interparticle separation was considered as the main contributing factor to the observed distinct differences in the *MH*-loops.

The two 3D systems compared here were fabricated from nominally the same building blocks. It was established that the average interparticle separation is different only by a small amount (~ 0.6 nm). Previous experimental results on ordered and disordered arrays of colloidal magnetic nanoparticles showed that decreasing the interparticle separation broadened the Zero Field Cooled (ZFC) curve,[2] but had only a slight effect on the remanence and coercivity.[1,2,15]

The results reported here show a dramatic change in coercivity and remanence when short range order/disorder is replaced by long range fcc order and there is only a small change in interparticle separation. Additionally we found that the *M-H* curve of the 3D periodic array at 273 K contains a hysteretic component, whereas the disordered array appears entirely superparamagnetic at the same temperature. This result, as well as ZFC magnetization and temperature dependences of magnetization, $M_s(T)$ and coercivity $H_c(T)$, needs a further investigation, which is underway.

IV. CONCLUSIONS

Crystalline and amorphous 3D assemblies of magnetic nanoparticles of Fe_3O_4-γ–Fe_2O_3, isolated and stabilized by protein apoferritin, were studied by SAXS and SANS. The spatial separations between nanoparticles in the two compared systems were found to be different only by a fraction of a nanometer. Nevertheless *M-H* curves, measured at 10 K, revealed significant differences: the coercivity and magnetic remanence are dramatically reduced for a crystalline assembly of nanoparticles in comparison with those for a disordered assembly, fabricated from nominally the same building blocks. We attribute these significant changes to the effect of nanoparticle ordering and collective behavior within the crystalline magnetic assembly.

ACKNOWLEDGMENTS

This work was supported by the Interdisciplinary Research Collaboration in Nanotechnology, funded by the UK Engineering and Physical Sciences Research Council (O.K.). This work utilized facilities (SAXS) of and was partly supported by Helmholtz Centre Berlin for Materials and Energy.

[1] D. Farrell, Y. Cheng, R. W. McCallum, M. Sachan, and S. Majetich, J. Phys. Chem. B **109**, 13409 (2005).
[2] I. Lisiecki, D. Parker, C. Salzemann, and M. P. Pileni, Chem. Mater. **19**, 4030 (2007).
[3] D. Kechrakos and K. N. Trohidou, Phys. Rev. B **58**, 12169 (1998).
[4] P. D. Mitchler, R. M. Roshko, E. dan Dahlberg, and B. M. Moskowitz, IEEE Trans. Magn. **35**, 2029 (1999).
[5] D. P. E. Dickson, S. A. Walton, S. Mann, and K. Wong, Nanostruct. Mater. **9**, 595 (1997).
[6] K. Wong, T. Douglas, S. Gider, D. D. Awschalom, and S. Mann, Chem. Mater. **10**, 279 (1998).
[7] J. W. Bulte, T. Douglas, S. Mann, R. B. Frankel, B. M. Moskowitz, R. A. Brooks, C. D. Baumgamer, J. Vymazal, M. Strub, and J. A. Frank, J. Magn. Reson. Imaging **4**, 497 (1994).
[8] P. Southern, A. P. Robinson, O. I. Kasyutich, B. Warne, A. Bewick, and W. Schwarzacher, J. Phys.: Condens. Matter **19**, 456204 (2007).
[9] Ó. Iglesias and A. Labarta, Phys. Rev. B **70**, 144401 (2004).
[10] O. Kasyutich, A. Sarua, and W. Schwarzacher, J. Phys. D **41**, 134022 (2008).
[11] W. Figueiredo and W. Schwarzacher, Phys. Rev. B **77**, 104419 (2008).
[12] C. F. Yavuz, J. T. Mayo, W. W. Yu, A. Prakash, J. C. Falkner, S. Yean, L. Cong, H. J. Shipley, A. Kan, M. Tomson, D. Natelson, and V. L. Colvin, Science **314**, 964 (2006).
[13] J. Als-Nielsen and D. McMorrow, *Elements of Modern X-Ray Physics* (Wiley, New York, 2001).
[14] D. I. Svergun and M. H. J. Koch, Rep. Prog. Phys. **66**, 1735 (2003).
[15] D. Farrell, Y. Cheng, Y. Ding, S. Yamamuro, C. Sanchez-Hanke, C. Kao, and S. Majetich, J. Magn. Magn. Mater. **282**, 1 (2004).